Reinforcement of the 400kV Scottish-English Interconnectors Using VSC-HVDC Transmission

Giddani O. A. Kalcon, Abdelaziz Y. M. Abbas, Grain P. Adam*

Sudan University of Science and Technology, School of Electrical and Nuclear Engineering, Khartoum, Sudan

*Electronic and Electrical Engineering Department, University of Strathclyde, Glasgow, UK

gidaniosman@sustech.edu; abdelaziz.abbas67@gmail.com; grain.adam@eee.strath.ac.uk

Abstract

This paper investigates the viability of using VSC-HVDC transmission to reinforce the existing HVAC Scottish- English interconnectors in an attempt to increase their power transfer capability without compromising network stability. Two reinforcement schemes are investigated: (1) decoupling the Scottish and English grids by converting the interconnectors into VSC-HVDC links, and (2) reinforcing the interconnectors with parallel VSC-HVDC links. The technical features of each scheme are demonstrated based on a generic model of the GB network implemented in Matlab/Simulink. Key simulation results are presented and discussed in detail.

Keywords

Power Management; Frequency Control; Reactive Power Compensation; VSC-HVDC

Nomenclature

HVDC	High-voltage direct current transmission
HVAC	High-voltage alternating current transmission
VSC	Voltage source converter
LCC	Line-commutated converter
FACTS	Flexible ac transmission systems
PCC	Point-of-common-coupling
GB	Great Britain

Introduction

The increased demand in electricity supply and aging power networks in Europe and the United States demand significant reinforcements to increase power transfer capability and enhance overall power system performance. VSC-HVDC transmission represents a suitable candidate to this aim due to its enhanced operation and controllability features (S. R. Pulikanti, *et al.* 2011, N. Flourentzou, *et al.* 2009, G. P. Adam, *et al.* 2010, M. Albaijat, *et al.* 2012, R. S. Balog, *et al.* 2012, K. N. Hasan, *et al.* 2011, L. Jiaqi, *et al.* 2012, A. Maknouninejad, *et al.* 2011, H. Mahmood, *et al.* 2012, R. Zhang, *et al.* 2010).

At present, the UK government has a target to increase the share of renewable energy to 20% by 2020 to meet its obligation to reduce CO_2 and other greenhouse gases emission. It is anticipated that onshore and offshore wind farms in the North and Northeast of Scotland will contribute to this in a significant proportion (O. A. Giddani, *et al.* 2010). However, to transfer bulk wind power from Scotland to the main load centers in England, will require reinforcing the two existing HVAC interconnectors between Scotland and England to increase their transmission capacity. There are three possible solutions being proposed at the moment (ENSG, UK, 2009, Z. Chengyong, *et al.* 2006, G. P. Adam, *et al.* 2010).

The first reinforcement solution is to increase the number of circuits, upgrade towers and insulation and to install FACTS devices (ENSG, UK, 2009, G. Chunyi, *et al.* 2010, D. Dong, *et al.* 2012, R. M. Gardner, *et al.* 2012, G. P. Adam, *et al.* 2010, D. Cuiqing, *et al.* 2008). This solution is less attractive today, mainly due to environmental concerns. The second solution is to convert the existing HVAC interconnectors into two overhead HVDC links using the existing towers and corridors. The main benefits of this approach are (G. Chunyi, *et al.* 2010, D. Dong, *et al.* 2012, S. Cole, *et al.* 2009, A. de la Villa Jaen, *et al.* 2008, C. Du, *et al.* 2009, S. Kouro, *et al.* 2010):

- Transmission capacity increases by 2.5 times.
- Voltage support at the Scottish and English grids may be achieved at no additional cost.
- Possibility of decoupling the Scottish and English grids, which may enhance overall power system stability.

The main drawback of this solution is that the effective inertia of the GB power network is reduced, and hence its natural ability to deal with frequency issues during

large disturbances (D. Dong, *et al.* 2012, A. Pizano-Martinez, *et al.* 2007, Z. Lidong, *et al.* 2011, F. A. R. Jowder, *et al.* 2004, D. L. H. Aik, *et al.* 1997).

The third solution is to reinforce the interconnectors with two parallel underground HVDC links. This approach does not compromise the effective inertia of the GB grid, and enhances the power flows in both networks. A drawback of this option is that a disturbance in one network may still propagate to the other (K. N. Hasan, et al. 2011, G. P. Adam, *et al.* 2010, D. Dong, *et al.* 2012, R. M. Gardner, *et al.* 2012, S. Kouro, *et al.* 2010, F. A. R. Jowder, *et al.* 2004).

This paper investigates the technical feasibility of implementing the second and third solutions. Their features and drawbacks are assessed regarding power control flexibility, provision of ancillary services, and resilience to ac network faults. A generic model of the GB network has been implemented in Matlab/ Simulink using detailed switch models of the HVDC neutral-point-clamped converters, synchronous machines and associated controllers, and dc and ac transmission lines.

Generic Model of the Great Britain Power Network

Fig. 1 shows the generic model of the GB power network implemented to carry out this investigation. The power transfer from Scotland to England is achieved via two HVAC links connected between buses B_8 and B_{10}, and B_9 and B_{11}. These links are known as the Western and Eastern interconnectors. The Scottish grid is represented by major generation plants, substations and 400kV transmission lines. Future offshore wind farms are connected to substation B_7. The English network is represented by two large aggregate power plants and static loads. All parameters used are taken from the Seven Year Statement issued by National Grid (Z. Huang, *et al.* 2003, The Grid Code).

Reinforcement by Converting the HVAC Interconnectors into VSC-HVDC Transmission Links

The capacity and controllability of the interconnectors could be increased by replacing the Eastern and Western HVAC interconnectors between B_8 and B_{10}, and B_9 and B_{11} with two VSC-HVDC links rated at 2150MW and 2400MW, with dc links extending over 8km and 65km respectively. Potential benefits of this solution are (O. A. Giddani, *et al.* 2010, ENSG, UK, 2009).

i. Increased transmission capacity at reduced foot-print.
ii. The VSC-HVDC links could provide frequency and damping support to both networks.
iii. Decoupled operation preserves the autonomy of both networks while exchanging active power; this may also prevent fault propagation.

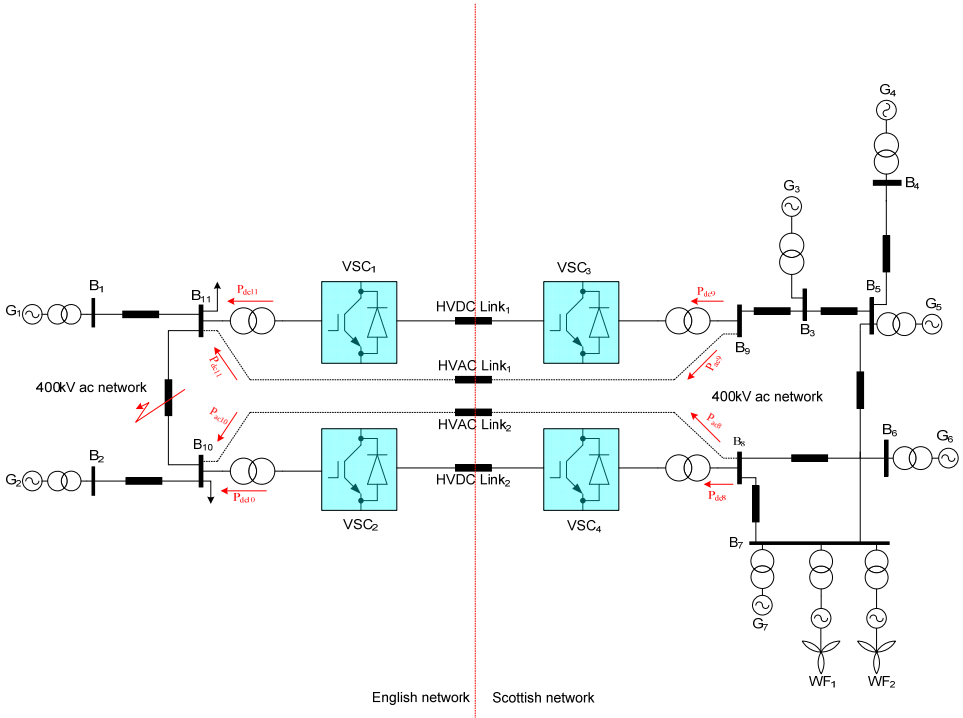

FIG. 1 SCOTTISH-ENGLISH INTERCONNECTORS' REINFORCEMENT SCENARIOS, (A) CONVERSION OF EXISTING HVAC LINKS INTO VSC-HVDC LINKS AND (B) REINFORCEMENT OF EXISTING HVAC LINKS WITH PARALLEL VSC-HVDC LINKS

The fast dynamic response of the VSC-HVDC links could improve frequency stability in the Scottish network and facilitate Grid Code compliance (ENSG, UK, 2009).

In this paper, converters VSC_1 and VSC_2 in Scotland are equipped with a basic active power controller to regulate the power flow to England plus an additional control loop to control the frequency in the Scottish grid, and an ac voltage controller to regulate the voltage at B_8 and B_9 as illustrated in Fig. 1. Converters VSC_3 and VSC_4 in England regulate the dc link voltage and the ac voltage at B_{10} and B_{11}. VSC_1 and VSC_2 monitor the frequency in the Scottish network and any difference from the nominal value activates the frequency controller generating a new power reference set-point that incorporates the effect of any active power mismatch. It is assumed that VSC_1 and VSC_2 can increase or decrease their output power by ±25% of the converter rating at any time without exceeding their current limits.

Reinforcement using Parallel HVAC-HVDC Links

This solution increases power transmission capacity between Scotland and England by adding two new point-to-point VSC-HVDC links in parallel with the existing HVAC links as shown in Fig. 1 and Fig. 2a. The added VSC-HVDC links could be used to improve utilization of the existing HVAC interconnectors using the reactive power capability of the VSC stations as shown in Fig. 2b. The VSC-HVDC converters are operated to regulate voltage at both ends of the HVAC links at 1.0 pu as shown in the vector diagram in Fig. 2b (which has been constructed assuming the power flow is from B_1 to B_3, the parallel ac lines are highly inductive, and the line stray capacitances are neglected). The active and reactive power exchange between converter VSC_1 and B_1 is:

$$\vec{I}_{c1} = \frac{\vec{V}_1 - \vec{V}_{c1}}{jX_{t1}} = \frac{1}{X_{t1}}\left[V_1 e^{-\frac{1}{2}\pi j} - V_{c1} e^{j(\delta_{c1}-\frac{1}{2}\pi)}\right] \quad (1)$$

$$P_{c1} + jQ_{c1} = \vec{V}_1 \vec{I}_{c1}^{*} = \frac{V_1^2}{X_{t1}} e^{j\frac{1}{2}\pi} - \frac{V_1 V_{c1}}{X_{t1}} e^{j(\frac{1}{2}\pi-\delta_{c1})} \quad (2)$$

$$P_{c1} = -\frac{V_1 V_{c1}}{X_{t1}} \sin\delta_{c1} \quad (3)$$

$$Q_{c1} = \frac{V_1^2}{X_{t1}} - \frac{V_1 V_{c1}}{X_{t1}} \cos\delta_{c1} \quad (4)$$

Similarly, the active and reactive power that converter VSC_3 exchanges with B_3 are (N. Flourentzou, *et al.* 2009):

$$P_{c3} = \frac{V_3 V_{c3}}{X_{t3}} \sin(\delta_{c3} - \delta_3) \quad (5)$$

$$Q_{c3} = \frac{V_3 V_{c3}}{X_{t3}} \cos(\delta_{c3} - \delta_3) - \frac{V_3^2}{X_{t3}} \quad (6)$$

The active and reactive power at the sending end of the HVAC line in parallel with the VSC-HVDC link is:

$$P_{ac1} = -\frac{V_1 V_3}{X_{13}} \sin\delta_3 \quad (7)$$

$$Q_{ac1} = \frac{V_1^2}{X_{13}} - \frac{V_1 V_3}{X_{13}} \cos\delta_3 \quad (8)$$

When VSC_1 and VSC_3 regulate the voltage at B_1 and B_3 such that $|\vec{V}_1| = |\vec{V}_3| = V_1$, the power factor at both ends of the HVAC line between B_1 and B_3 will be the same and given by $\cos\varphi_{ac1} = \cos\varphi_{ac3} = \cos\frac{1}{2}\delta_3$ as illustrated in Fig. 2b. This case is identical to that when the line is fully compensated with an SVC or a STATCOM at the middle. This demonstrates the technical and economic value of the parallel scheme especially in the context of network reinforcement and offshore wind farm connection.

Since VSC_1 and VSC_2 regulate $V_1 = V_3$, then $\frac{1}{2} I_{12} X_{12} = V_1 \sin\varphi_{ac1} = V_2 \sin\varphi_{ac2} = V_1 \sin\frac{1}{2}\delta_2$, the active and reactive power at the sending end can be expressed as:

$$P_{ac1} = -\frac{V_1^2}{X_{12}} \sin\delta_2 \quad (9)$$

$$Q_{ac1} = \frac{2V_1^2}{X_{12}} \sin^2\tfrac{1}{2}\delta_2 = \tfrac{1}{2} X_{12} I_{ac1}^2 \quad (10)$$

The vector diagrams in Figs. 2b and 2c show the operating regions of both converter stations during power transmission from B_1 to B_3, including zero and unity power factor boundaries, and the regions where converter operation is limited by available dc link voltage and converter switching device current rating. Fig. 2c shows that changing the VSC operation from over-excitation (i.e. VSC releases VAr to the ac network), to under-excitation (i.e. VSC absorbs VAr from the ac network), the voltage vector $\vec{V}_c$ moves from the purple region, through the unity power factor boundary line, into the light-green region. While power reversal requires movement of vector, $\vec{V}_c$, through the zero power factor boundary line. The reinforcement solution using a hybrid connection, increases transmission capacity without decoupling the two networks.

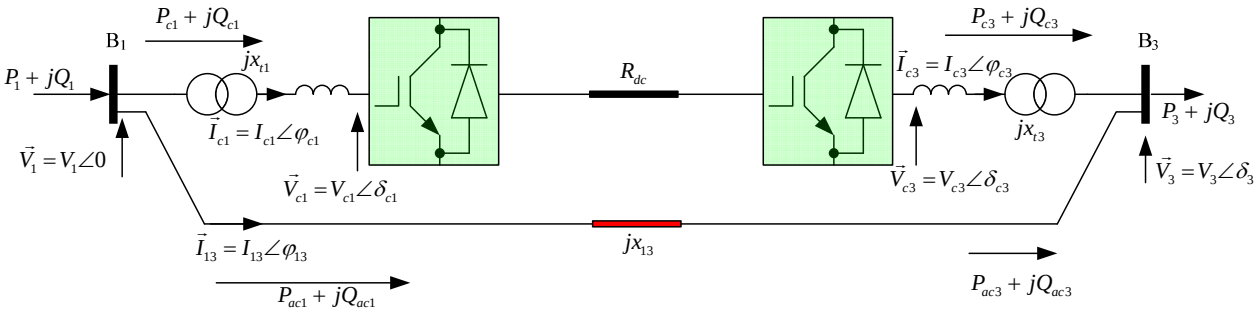

(a) Single-line diagram of VSC-HVDC1 and HVAC1 lines connecting buses B9 and B11 in Fig.1

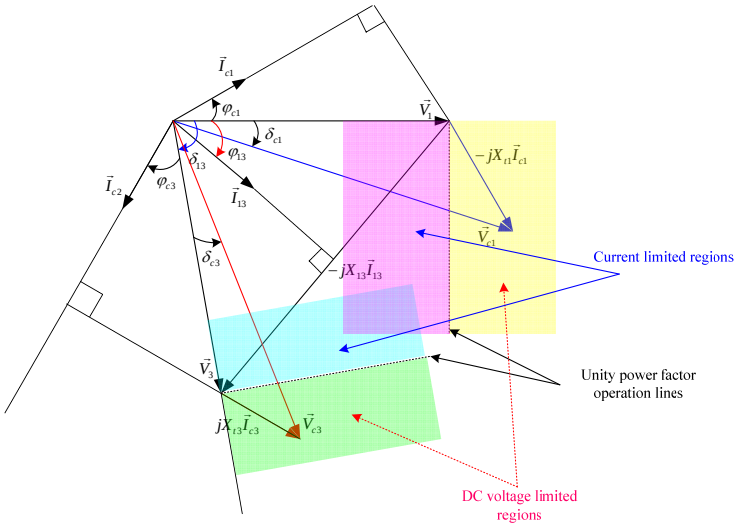

(b) Phasor diagram of hybrid connecting two ac systems

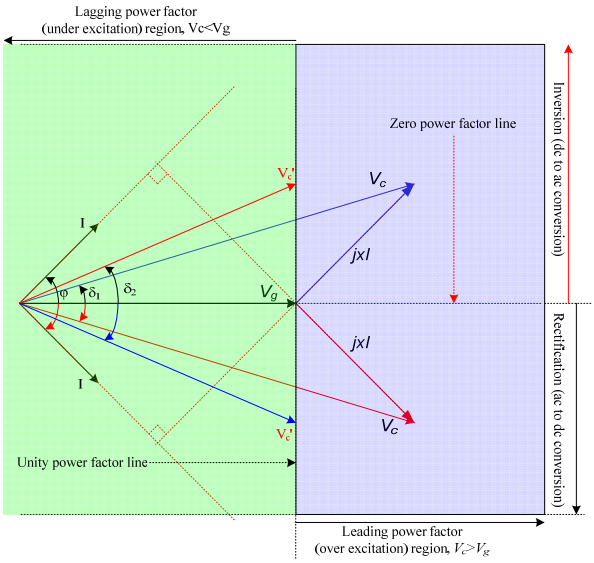

(c) Phasor diagram depicts active and reactive power control of voltage source converter and their limits

FIG. 2 ILLUSTRATIVE MODEL OF THE HYBRID PARALLEL INTERCONNECTOR BETWEEN B1 AND B3AND ITS VECTOR DIAGRAM

Also, this solution may prevent undesired power flow loops as converters VSC1 and VSC3 set the voltage at B1 and B3 to be $|\vec{V}_1| = |\vec{V}_3|$, and force $\vec{V}_1$ to advance $\vec{V}_3$ in order to allow power flow from B1 and B3.

System Modeling

In this paper, converters VSC1 through VSC4 are neutral-point-clamped (NPC) converters and detailed switch models, including capacitor voltage balancing and associated controllers have been used. All converters are controlled using carrier-based sinusoidal pulse-width modulation (SPWM), with 2kHz switching frequency. Fig. 3 summarizes the basic controllers for the HVDC link (ac current, active power, dc voltage, ac voltage, and frequency). The voltage balance of the two dc link capacitors of each NPC converter is maintained using the well-established dc-offset method. The VSC current controller is designed in the dq synchronous reference frame rotating at speed ω_0. Based on Fig. 3, the differential equation describing the VSC ac side dynamics is:

$$V_{cdq} = RI_{dq} + L\frac{dI_{dq}}{dt} + j\omega_0 LI_{dq} + V_{dq} \quad (11)$$

where $V_{cdq} = V_{cd} + jV_{cq}$, $I_{dq} = I_d + jI_q$, and $V_{dq} = V_d + jV_q$

$$\frac{dI_{dq}}{dt} = -\frac{R}{L}I_{dq} + \frac{V_{cdq} - j\omega_0 L - V_{dq}}{L} = -\frac{R}{L}I_{dq} + \frac{U_{dq}}{L} \quad (12)$$

The current controller regulates the ac current by estimating the converter terminal voltage using

$$V_{cdq} = U_{dq} + j\omega LI_{dq} + V_{dq} \quad (13)$$

where U_{dq} represents the output of the proportional integral controller given as:

$$U_{dq} = k_{pi}(I_{dq}^* - I_{dq}) + k_{ii}\int(I_{dq}^* - I_{dq})dt = k_{pi}(I_{dq}^* - I_{dq}) + Z_{dq} \quad (14)$$

where $U_{dq} = U_d + jU_q$ and $Z_{dq} = Z_d + jZ_q$

After rearrangement of (12) and (13), the following first-order differential equations are obtained:

$$\frac{dI_{dq}}{dt} = -\frac{(R + k_{pi})}{L}I_{dq} + \frac{Z_{dq}}{L} + \frac{I_{dq}^*}{L} \quad (15)$$

$$\frac{dZ_{dq}}{dt} = k_{ii}(I_{dq}^{*} - I_{dq}) \tag{16}$$

After Laplace manipulation of (15) and (16), the following closed-loop transfer function is obtained:

$$\frac{I_{dq}(s)}{I_{dq}^{*}(s)} = \frac{\frac{k_{pi}}{L}s + \frac{k_{ii}}{L}}{s^2 + \frac{(k_{pi}+R)}{L}s + \frac{k_{ii}}{L}} \tag{17}$$

The proportional and integral gains of the current controller are defined to achieve appropriate settling time and damping ratio, ζ (and then the natural frequency ω_n is calculated). Therefore, the gains are: $k_{pi} = 2\zeta\omega_n L - R$ and $k_{ii} = \omega_n^2 L$

The dc voltage controller regulates the dc voltage by estimating the reference active current component required to inject the power available in the dc side into the ac side (keeping the power balance). This is achieved by estimating the dc link capacitor current as follow:

$$C\frac{dV_{dc}}{dt} = I_{dc} - I_i \tag{18}$$

$$U_{dc} = I_{dc} - I_i = k_{pdc}(V_{dc}^{*} - V_{dc}) + k_{idc}\int(V_{dc}^{*} - V_{dc})dt \tag{19}$$

where $Z_{dc} = k_{idc}\int(V_{dc}^{*} - V_{dc})dt$

After algebraic manipulation and rearrangement of (18) and (19):

$$\frac{dV_{dc}}{dt} = \frac{-k_{pdc}}{C}V_{dc} + \frac{1}{C}Z_{dc} + \frac{1}{C}V_{dc}^{*} \tag{20}$$

$$\frac{dZ_{dc}}{dt} = k_{idc}(V_{dc}^{*} - V_{dc}) \tag{21}$$

After applying Laplace transformation to (20) and (21), the following transfer function is obtained:

$$\frac{V_{dc}(s)}{V_{dc}^{*}(s)} = \frac{\frac{k_{pdc}}{C}s + \frac{k_{idc}}{C}}{s^2 + \frac{k_{pdc}}{C}s + \frac{k_{idc}}{C}} = \frac{1}{\alpha_c s + 1} \tag{22}$$

By forcing the dc voltage transfer function to be of first order with unity gain and time constant of α_c, the following gains are obtained: $k_{pdc} = \frac{C}{\alpha}$ and $k_{idc} = 0$.

It can be noticed that proportional control may be sufficient to control the dc voltage. Such design approach is appropriate for the dc voltage controller as its natural dynamics are much slower than those of the ac current, which is controlled by the inner controller. Based on (19), and assuming the dc to ac conversion process is lossless, the reference active current component is:

$$I_d^{*} = \frac{(I_{dc} - U_{dc}) \times V_{dc}}{V_d^{*}} \tag{23}$$

For the ac voltage controller, the reactive power that the converter exchanges at the PCC to regulate the voltage is:

$$Q^{*} = k_{pv}(|V_{ac}^{*}| - |V_{ac}|) + k_{iv}(|V_{ac}^{*}| - |V_{ac}|) \tag{24}$$

The reactive current reference for the current controller is obtained as:

$$I_q^{*} = -\frac{Q^{*}}{|V_d^{*}|} = -\frac{Q^{*}}{|V_{ac}^{*}|} \tag{25}$$

The frequency controller in Fig. 3 could be designed based on an equation similar to that of the dc voltage controller. Hence, the relationship between ac and dc power can be expressed as:

$$CV_{dc0}\frac{dV_{dc}}{dt} = (I_{dc} - I_i) \times V_{dc0} = P_{dc} - P_{ac} \tag{26}$$

If the converter is rated at S_0 MVA, the dc link voltage V_{dc0} of (26) can be written as

$$\frac{2}{V_{dc0}} \times \frac{\frac{1}{2}CV_{dc0}^2}{S_0}\frac{dV_{dc}}{dt} = \frac{P_{dc} - P_{ac}}{S_0} = \overline{\Delta P} \tag{27}$$

$$\frac{2H_1}{V_{dc0}} \times \frac{dV_{dc}}{dt} = \overline{\Delta P} \tag{28}$$

where $H_1 = \frac{\frac{1}{2}CV_{dc0}^2}{S_0}$ represents the converter *inertia constant* in secs, and $\overline{\Delta P}$ represents the per unit active power mismatch between the ac and dc sides. It can be observed that (28) describes the amount of active power mismatch that may be needed to influence the ac network frequency in terms of the rate-of-change in the dc link voltage and converter inertia. To facilitate the design of the frequency controller, assume that the ac network has an equivalent inertia constant of H_2, then the swing equation for the ac side can be expressed in terms of the ac network frequency as follow:

$$\frac{2H_2}{\omega_0} \times \frac{d\omega}{dt} = \frac{2H_2}{f_0} \times \frac{df}{dt} = \overline{\Delta P} \tag{29}$$

Since (28) and (29) are equivalent, (29) will be used to design the frequency controller. $\overline{\Delta P}$ can be obtained from a simple PI controller as:

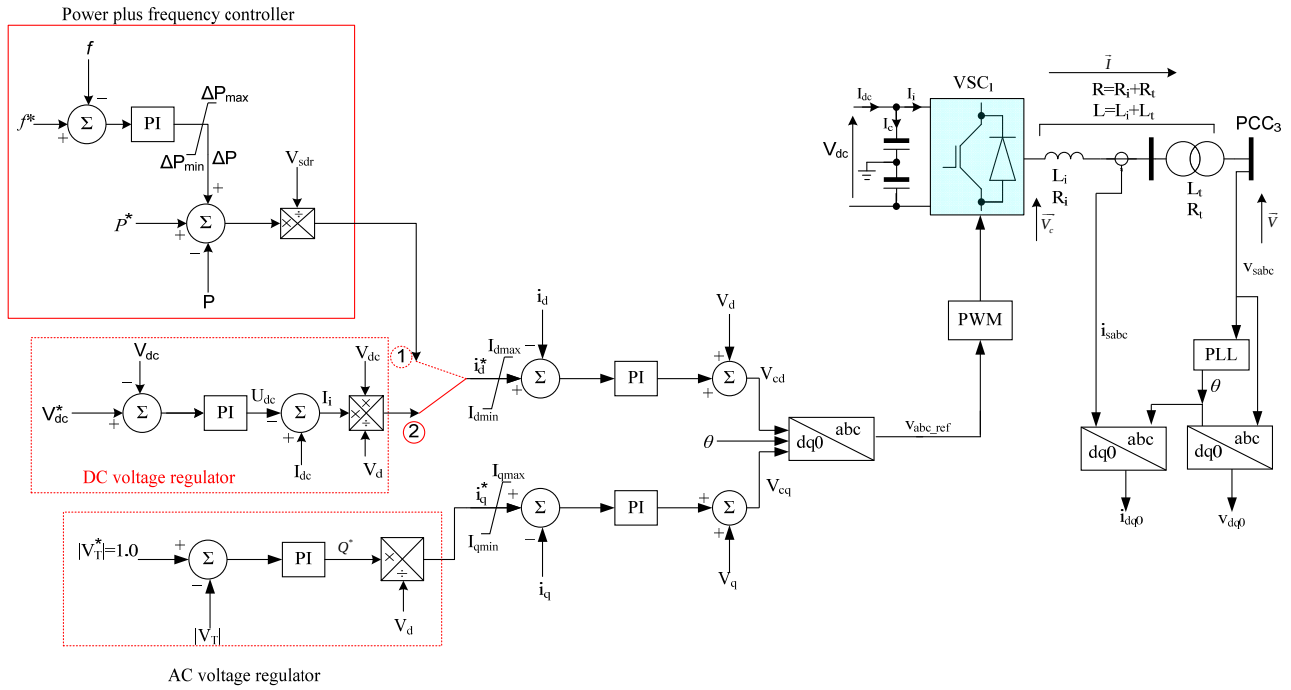

FIG. 3 GENERIC BLOCK DIAGRAM OF THE VSC-HVDC CONTROLLERS PLUS CONTROL LOOP TO PROVIDE FREQUENCY SUPPORT

$$\Delta P = k_{pf}(f^* - f) + k_{if}\int(f^* - f)dt \quad (30)$$

where k_{pf} and k_{if} are the proportional and integral gains of the frequency controller.

$$\Delta P = k_{pf}(f^* - f) + Z_f \quad (31)$$

After algebraic manipulation of (29), (30) and (31), the following differential equations are obtained:

$$\frac{df}{dt} = \frac{f_0}{2H_2}\left[k_{pf}(f^* - f) + Z_f\right] \quad (32)$$

$$\frac{dZ_f}{dt} = k_{if}(f^* - f) \quad (33)$$

After Laplace manipulation of (32) and (33), the following transfer function is obtained:

$$\frac{f(s)}{f^*(s)} = \frac{f_0}{2H} \times \frac{k_{pf}s + k_{if}}{s^2 + \frac{k_{pf}f_0}{2H}s + \frac{k_{if}f_0}{2H}} \quad (34)$$

Using the same procedure adopted for selecting the current controller gains, the frequency controller gains are obtained as follow: $k_{pf} = \frac{4\zeta\omega_n H}{f_0}$ and $k_{if} = \frac{2\omega_n^2 H}{f_0}$

Simulations

Decoupled Operation of the Scottish and English Transmission Networks

To facilitate the assessment of this reinforcement option the GB transmission network in Fig. 2 is simulated with converters VSC_3 and VSC_4 regulating the active power export to England and the Scottish network frequency (see Fig. 3). These converters also control the ac voltage at B_8 and B_9. VSC_1 and VSC_2 regulate their dc link voltage and the ac voltage at B_{10} and B_{11}. Fig. 4 compares two simulation results obtained when a major load of 500+j100 MVA is connected to the Scottish grid at t=5s, with and without frequency control loop in VSC_3 and VSC_4. It can be noted that with the frequency control loop the frequency in the Scottish grid is restored faster to its pre-disturbance nominal value than without this additional control loop as shown in Fig. 4a. It can be noticed that the frequency controllers sense the decrease in the Scottish network frequency and generate a negative correction signal to reduce the power transmitted to England by an amount exactly enough to stabilize the network frequency, as shown in Fig. 4b and Fig 4c.

Figs. 4b to 4d show that converters VSC_1 to VSC_4 perform fast power run-down in an attempt to maintain the power balance in the Scottish network. VSC_1 and VSC_2 adjust the transmitted power from 2150MW to 1970MW and from 2400MW to 2200MW respectively. This represents an adjustment of 72% of the power mismatch, with the conventional generation units in Scotland (SG1-to-SG5) covering the remaining 28%. Fig. 4f shows the voltage magnitude at the PCCs (buses B_8 and B_{11}), which is maintained at 1.0pu.

Fig. 5 shows the key responses in the case of over-generation due to the loss of a major load in

Scotland, 500+j100 MVA, where VSC_3 and VSC_4 perform fast power ramp-up to maintain the power balance in the Scottish network (Figs. 5b through 5d. It can be observed that the frequency in the Scottish network is restored faster to its nominal value with the frequency controller at VSC_3 and VSC_4 in operation. These results demonstrate that the decoupled operation of the Scottish and English networks improves the overall power system and voltage stability, allows frequency stabilization in the Scottish grid, and enhances power transfer capacity.

To demonstrate the benefits of the decoupled operation in the event of a fault, a three-phase fault is applied at the middle of the line connecting buses B_{10} and B_{11} in England, with 200 msec fault duration (see Fig. 1). In this case, the voltage at B_{10} and B_{11} collapses and the power transfer capability of VSC_1 and VSC_3 reduces. This causes a rise in the dc link voltage, which is minimised here by tailoring the active powers at the sending-end converters such that $P_8^* = P_8^0 \times \frac{V_{10}}{V_{10}^0}$ and $P_9^* = P_9^0 \times \frac{V_{11}}{V_{11}^0}$. P_8^0 and P_9^0 represent pre-fault power set-points to VSC_4 and VSC_3; V_{10}^0 and V_{11}^0, V_{10} and V_{11} are the nominal and actual voltage magnitudes at B_{10} and B_{11}.

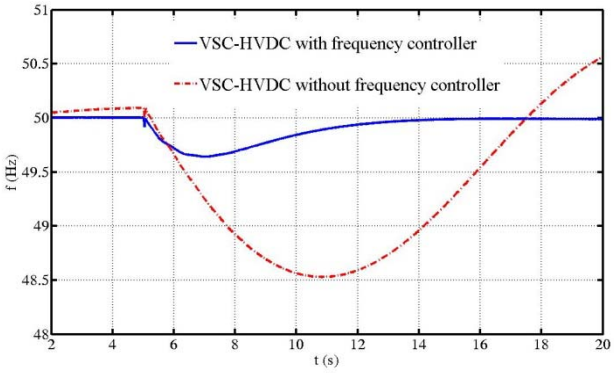

(a) Frequency in the Scotland network

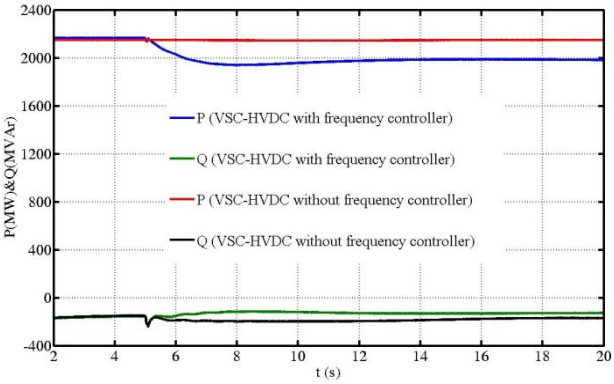

(b) Active and reactive power VSC_4 exchange with B_8 (sending end)

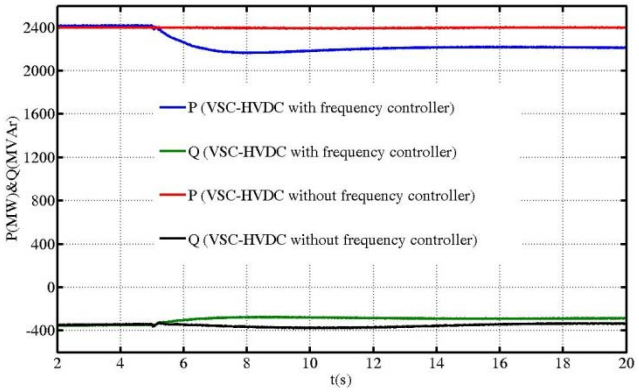

(c) Active and reactive power VSC_3 exchange with B_9 (sending end)

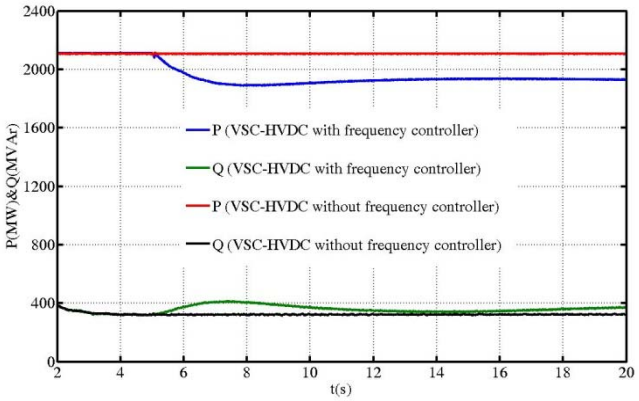

(d) Active and reactive power VSC_1 exchange with B_{11} at the

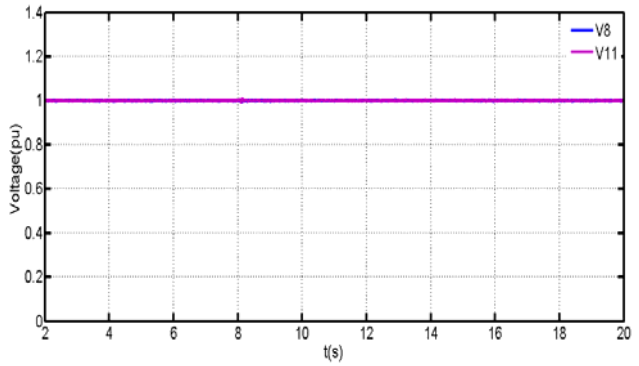

(e) The voltages at busses B_1-B_4

FIG. 4 DECOUPLED OPERATION TO FREQUENCY SUPPORT IN SCOTTISH NETWORK (INTRODUCTORY OF 500+J100 MVA AT TIME T=5S)

Figs. 6a and 6c show the active and reactive power exchanged by the sending- and receiving-end converters with theirs PCCs. Fig. 6b shows that the voltage at B_8 and B_9 in Scotland are not affected by the fault in England despite the significant voltage drop at B_{10} and B_{11} as shown in Fig. 6d. Fig. 6e shows the converter VSC_4 current waveforms. The reduction seen in the VSC_4 current is due to the tailoring of the power commands in VSC_3 and VSC_4 to reduce the *dv/dt* and voltage stresses on converter switches. It can also be noted that converter VSC_2 contributes limited current to the fault.

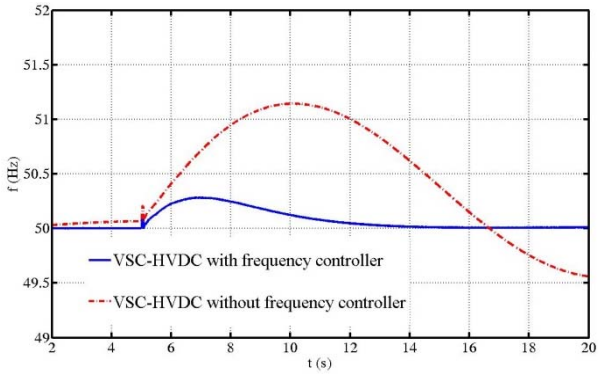

(a) Frequency in the Scotland network

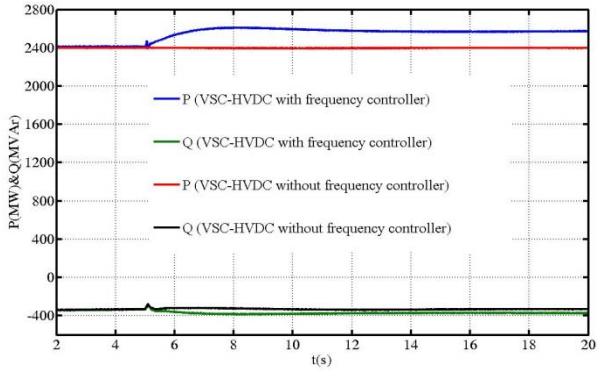

(b) Active and reactive power of VSC_4 exchange with B_8 (sending end)

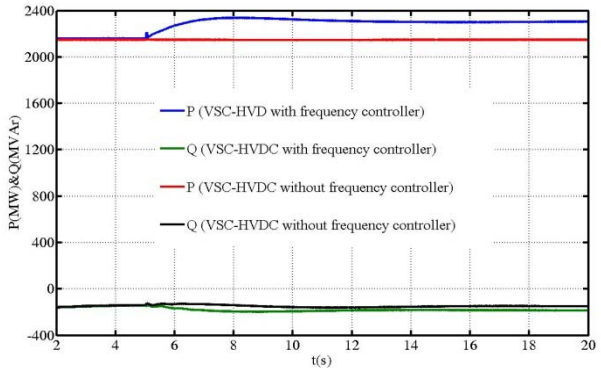

(c) Active and reactive power of VSC3 exchange with B_9 (sending end)

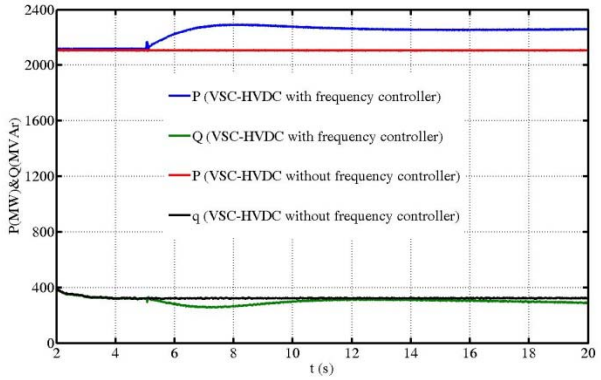

(d) Active and reactive power VSC_1 exchange with B_{11}

FIG. 5 WAVEFORMS ILLUSTRATING THE POTENTIAL BENEFIT OF DECOUPLED OPERATION TO FREQUENCY SUPPORT IN SCOTTISH NETWORK (INTRODUCTORY OF 500+J100 MVA AT TIME T=5S)

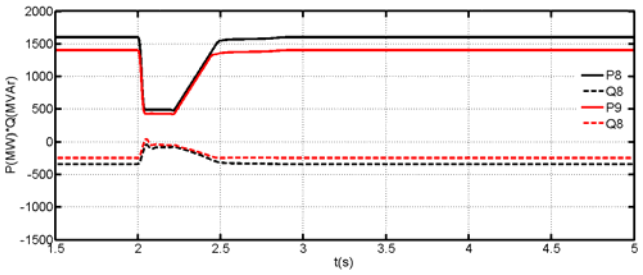

(a) Active and reactive sending end converters VSC_4 and VSC_3 exchange with B_8 and B_9

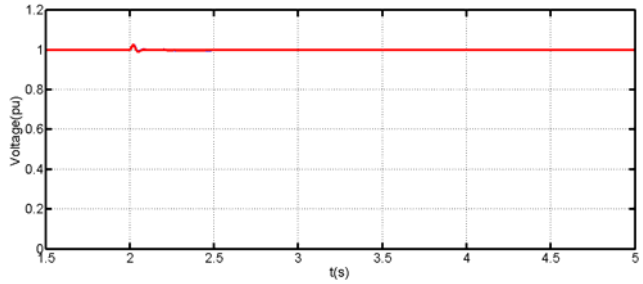

(b) Voltage magnitude at B_8 and B_9

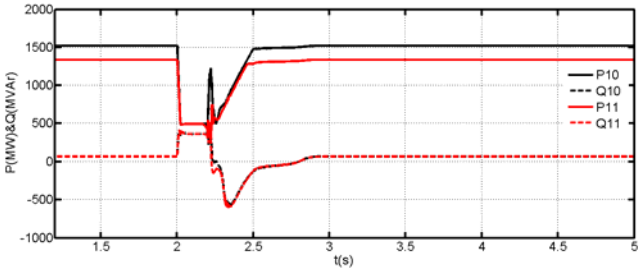

(c) Active and reactive power receiving end converters exchange with B_{10} and B_{11}

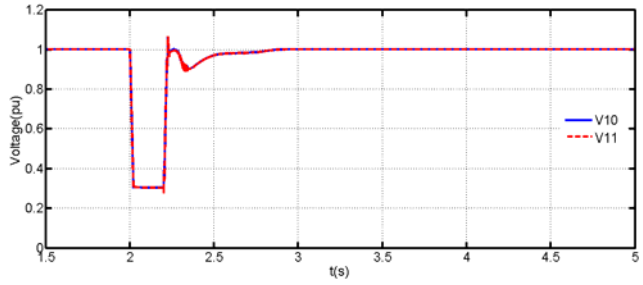

(d) Voltage magnitude at B_{10} and B_{11}

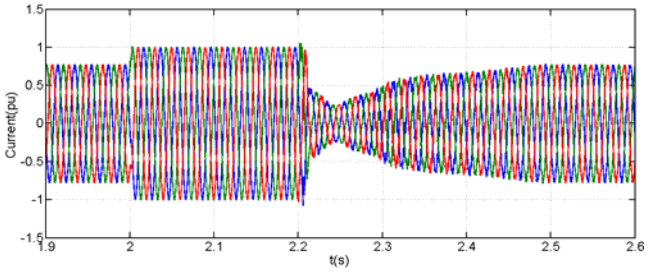

(e) Current waveforms converter VSC_2 exchanges with B_{10}

FIG. 6 WAVEFORMS DEMONSTRATING PREVENTION OF UNINTENDED FAULT PROPAGATION IN VSC-HVDC

Hybrid Connection

This section assesses the reinforcement option where VSC-HVDC links are connected in parallel with

existing HVAC interconnectors between B_8 and B_{10}, and B_9 and B_{11} as illustrated in Fig. 1. In this case, converters VSC_3 and VSC_4 export 1.0 GW and 1.2 GW to England, respectively, and regulate the ac voltage at B_8 and B_9 at 1.0 pu. Converters VSC_1 and VSC_2 regulate their dc link voltage at 300 kV, and maintain the voltage magnitude at B_{10} and B_{11} at 1.0pu. In order to examine the transient response a three-phase fault is applied at t=3 sec in the England network in the line connecting buses B_{10} and B_{11}, 30 km from B_{10}, with 200msec fault duration. At t=8sec, converter VSC_4 is commanded to increase its power export to England through the VSC-HVDC link connected between B_9 and B_{11} to 1.4 GW.

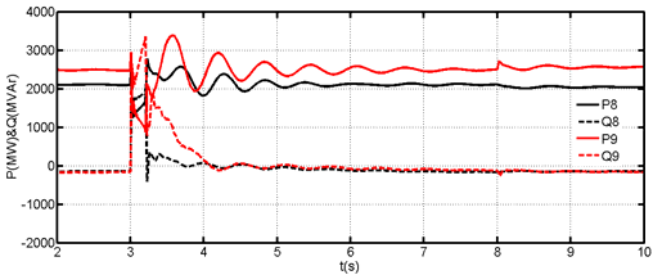

(a) Total active and reactive power at the send ends of the Eastern and Western interconnectors, including ac and dc links

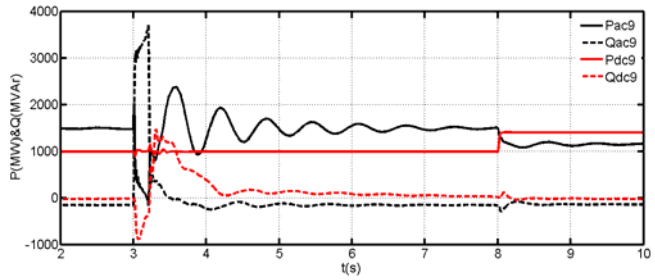

(b) Active and reactive power at the sending ends of HVAC and VSC-HVDC links connected between B9 and B11

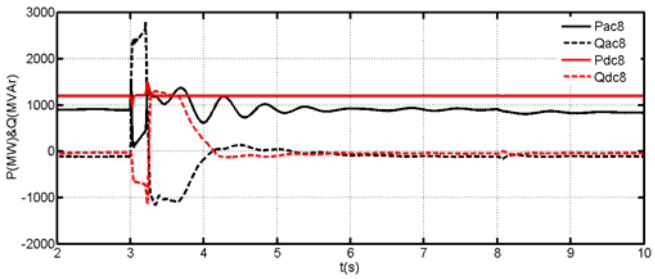

(c) Active and reactive power at the sending ends of HVAC and VSC-HVDC links connected between B_8 and B_{10} (P_{ac8}+jQ_{ac8} and P_{dc8}+jQ_{dc8})

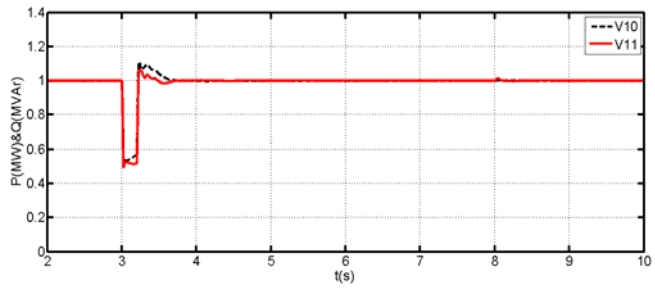

(d) Voltage magnitude at B10 and B11

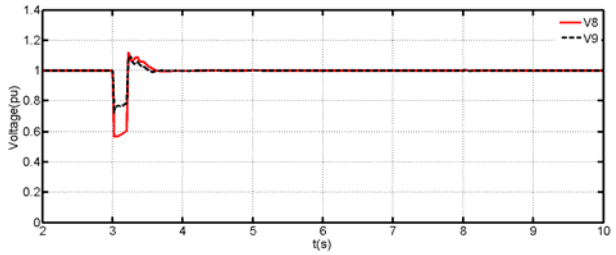

(e) Voltage magnitude at B8 and B9

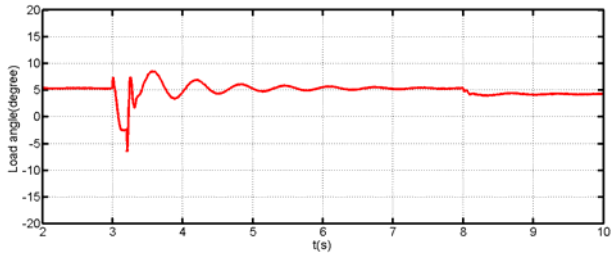

(f) Load angle δ_{11}-δ_9

FIG. 7 KEY WAVEFORMS SHOWING THE GB NETWORK RESPONSE DURING AC FAULTS WITH THE HYBRID REINFORCEMENT SCHEME

Fig. 7a shows the combined powers of the HVAC plus VSC-HVDC links connected between B_8 and B_{10}, and B_9 and B_{11}, monitored at the sending-end buses B_8 and B_9. Figs. 7b and 7c show the power sharing between the HVAC and VSC-HVDC links of the Eastern and Western interconnectors between B_8 and B_{10}, and B_9 and B_{11}, monitored at the sending-end buses B_8 and B_9. It can be observed that the change in the power set-point of the converter that controls the power export in the VSC-HVDC link between B_9 and B_{11} does not vary the total power exported to England through Western interconnector, instead it varies the power transmitted through its neighbouring HVAC link. Figs. 7d and 7e show that the voltage at buses B_8 and B_9, and B_{10} and B_{11} are regulated at 1.0pu in steady-state. The converters of the VSC-HVDC links adjust their reactive power to support the voltage at these busses during the fault as shown in Figs. 7b and 7c. Fig. 7f shows that the voltage angle of bus B_{11} relative to B_9, δ_{11}-δ_9, varies with loading of the HVAC link, as expected. It is important to note that power flow loops can be prevented as long as the voltage at sending-end advances that of the receiving-end, whilst both are regulated at 1.0 pu.

Conclusions

This paper investigated two possible reinforcement solutions for the existing Eastern and Western HVAC interconnectors between Scotland and England using VSC-HVDC transmission. The first reinforcement solution proposes converting the existing HVAC interconnectors into VSC-HVDC links. This solution resulted in the asynchronous connection of the Scottish

and English networks, which may prevent fault propagation and facilitate increased connection of renewable in the GB network, benefiting from the fast dynamic response of the VSC-HVDC links and large size of the English network. The second reinforcement solution proposed a hybrid scheme where VSC-HVC links are connected in parallel with the existing HVAC interconnectors. It was found that this solution increases power transmission capacity at the expense of increased footprint and reduced losses in the ac links, prevents power flow loops and improves the voltage stability of both networks. However, it results in synchronous connection of the Scottish and English networks; hence frequency regulation and power balancing must still be performed by conventional plant.

REFERENCES

A. de la Villa Jaen, E. Acha, and A. G. Exposito, "Voltage Source Converter Modeling for Power System State Estimation: STATCOM and VSC-HVDC," *Power Systems, IEEE Transactions on,* vol. 23, pp. 1552-1559, 2008.

A. Maknouninejad, N. Kutkut, I. Batarseh, and Q. Zhihua, "Analysis and control of PV inverters operating in VAR mode at night," in *Innovative Smart Grid Technologies (ISGT), 2011 IEEE PES*, 2011, pp. 1-5.

A. Pizano-Martinez, C. R. Fuerte-Esquivel, H. Ambriz-Perez, and E. Acha, "Modeling of VSC-Based HVDC Systems for a Newton-Raphson OPF Algorithm," *Power Systems, IEEE Transactions on,* vol. 22, pp. 1794-1803, 2007.

C. Du, E. Agneholm, and G. Olsson, "VSC-HVDC System for Industrial Plants With Onsite Generators," *Power Delivery, IEEE Transactions on,* vol. 24, pp. 1359-1366, 2009.

D. Cuiqing, E. Agneholm, and G. Olsson, "Use of VSC-HVDC for Industrial Systems Having Onsite Generation With Frequency Control," *Power Delivery, IEEE Transactions on,* vol. 23, pp. 2233-2240, 2008.

D. Dong, T. Thacker, I. Cvetkovic, R. Burgos, D. Boroyevich, F. F. Wang, and G. Skutt, "Modes of Operation and System-Level Control of Single-Phase Bidirectional PWM Converter for Microgrid Systems," *Smart Grid, IEEE Transactions on,* vol. 3, pp. 93-104, 2012.

D. L. H. Aik and G. Andersson, "Voltage stability analysis of multi-infeed HVDC systems," *Power Delivery, IEEE Transactions on,* vol. 12, pp. 1309-1318, 1997.

Electricity Networks Strategy Group, (ENSG) "OUR ELECTRICITY TRANSMISSION NETWORK:A VISION FOR 2020", UK2009.

F. A. R. Jowder and O. Boon Teck, "VSC-HVDC station with SSSC characteristics," *Power Electronics, IEEE Transactions on,* vol. 19, pp. 1053-1059, 2004.

G. Chunyi and Z. Chengyong, "Supply of an Entirely Passive AC Network Through a Double-Infeed HVDC System," *Power Electronics, IEEE Transactions on,* vol. 25, pp. 2835-2841, 2010.

G. P. Adam, S. J. Finney, B. W. Williams, K. Bell, and G. M. Burt, "Control of multi-terminal DC transmission system based on voltage source converters," in *AC and DC Power Transmission, 2010. ACDC. 9th IET International Conference on*, 2010, pp. 1-5.

G. P. Adam, S. J. Finney, B. W. Williams, D. R. Trainer, C. D. M. Oates, and D. R. Critchley, "Network fault tolerant voltage-source-converters for high-voltage applications," in *AC and DC Power Transmission, 2010. ACDC. 9th IET International Conference on*, 2010.

G. P. Adam, K. H. Ahmed, S. J. Finney, and B. W. Williams, "AC fault ride-through capability of a VSC-HVDC transmission systems," in *Energy Conversion Congress and Exposition (ECCE), 2010 IEEE*, 2010.

H. Mahmood and J. Jin, "Modeling and Control System Design of a Grid Connected VSC Considering the Effect of the Interface Transformer Type," *Smart Grid, IEEE Transactions on,* vol. 3, pp. 122-134, 2012.

K. N. Hasan, T. K. Saha, and M. Eghbal, "Renewable power penetration to remote grid - transmission configuration and net benefit analyses," in *Innovative Smart Grid Technologies Asia (ISGT), 2011 IEEE PES*, 2011, pp. 1-8.

L. Jiaqi, G. K. Venayagamoorthy, and R. G. Harley, "Wide-Area Measurement Based Dynamic Stochastic Optimal Power Flow Control for Smart Grids With High Variability and Uncertainty," *Smart Grid, IEEE Transactions on,* vol. 3, pp. 59-69, 2012.

M. Albaijat, K. Aflaki, and B. Mukherjee, "Congestion management in WECC grid," in *Innovative Smart Grid Technologies (ISGT), 2012 IEEE PES*, 2012, pp. 1-8

N. Flourentzou, V. G. Agelidis, and G. D. Demetriades, "VSC-Based HVDC Power Transmission Systems: An Overview," *Power Electronics, IEEE Transactions on*, vol. 24, pp. 592-602, 2009.

O. A. Giddani, G. P. Adam, O. Anaya-Lara, G. Burt, and K. L. Lo, "Potential benefits of decoupling the Scotland-England network using VSC-HVDC," in *AC and DC Power Transmission, 2010. ACDC. 9th IET International Conference on*, 2010, pp. 1-5.

R. S. Balog, W. W. Weaver, and P. T. Krein, "The Load as an Energy Asset in a Distributed DC SmartGrid Architecture," *Smart Grid, IEEE Transactions on,* vol. 3, pp. 253-260, 2012.

R. M. Gardner and L. Yilu, "Generation-Load Mismatch Detection and Analysis," *Smart Grid, IEEE Transactions on,* vol. 3, pp. 105-112, 2012.

R. Zhang, Y. Du, and L. Yuhong, "New challenges to power system planning and operation of smart grid development in China," in *Power System Technology (POWERCON), International Conference on*, 2010.

S. Cole and R. Belmans, "Transmission of bulk power," *Industrial Electronics Magazine, IEEE,* vol. 3, pp. 19-24, 2009.

S. Kouro, M. Malinowski, K. Gopakumar, J. Pou, L. G. Franquelo, W. Bin, J. Rodriguez, Pe, x, M. A. rez, and J. I. Leon, "Recent Advances and Industrial Applications of Multilevel Converters," Industrial Electronics, IEEE Transactions on, vol. 57, pp. 2553-2580, 2010.

S. R. Pulikanti and V. G. Agelidis, "Hybrid Flying-Capacitor-Based Active-Neutral-Point-Clamped Five-Level Converter Operated With SHE-PWM," *Industrial Electronics, IEEE Transactions on,* vol. 58, pp. 4643-4653, 2011.

The Grid Code, Issue 3, Revision 12, vol. National GridElectricity Transmission plc.7 avialable at http://www.nationalgrid.com/uk/Electricity/Codes/gridcode/gridcodedocs/.

Z. Chengyong and S. Ying, "Study on Control Strategies to Improve the Stability of Multi-Infeed HVDC Systems Applying VSC-HVDC," in *Electrical and Computer Engineering, 2006. CCECE '06. Canadian Conference on*, 2006, pp. 2253-2257.

Z. Huang, B. T. Ooi, L. A. Dessaint, and F. D. Galiana, "Exploiting voltage support of voltage-source HVDC," *Generation, Transmission and Distribution, IEE Proceedings-,* vol. 150, pp. 252-256, 2003.

Z. Lidong, L. Harnefors, and H. P. Nee, "Interconnection of Two Very Weak AC Systems by VSC-HVDC Links Using Power-Synchronization Control," *Power Systems, IEEE Transactions on,* vol. 26, pp. 344-355, 2011.

Giddani O. A. Kalcon received the B.Eng degree (in honors) in power system and machines from Sudan University of Science and Technology (SUST), Sudan, in 2001, and the M.Sc degree in electrical power system from SUST, and the Ph.D. degree in advanced power engineering from Strathclyde University, Glasgow, U.K., in 2011. He is currently with the School of Electrical and Nuclear Engineering, Sudan University of Science and Technology, his research interest include wind farm power integration and HVDC transmission system.

Abdelaziz Yousif Mohamed Abbas received the B. Tech. (First class Honors) and M.Sc. degrees from the Sudan University of Science and Technology, Khartoum, Sudan, in 1996 and 2002, respectively, and the Ph.D. degree from Strathclyde University, Glasgow, U.K., in 2009, all in electrical and electronic engineering. From 1996 to 2005, he was a Teaching Assistant then a Lecturer with Sudan University of Science and Technology, where he is currently an Assistant Professor. His research interests include power electronics, drives and energy conversion, power quality and renewable integration, power systems operation and power systems stability and control. Dr. Abbas is a member of the Institution of Engineering and Technology.

Grain P. Adam received the first-class B.Sc. and M.Sc. degrees in electrical machines and power systems from Sudan University of Science and Technology, Khartoum, Sudan, in 1998 and 2002, respectively, and the Ph.D. degree in power electronics from Strathclyde University, Glasgow, U.K., in 2007. He is currently with the Department of Electronic and Electrical Engineering, Strathclyde University, and his research interests are multilevel inverters, electrical machines and power systems control and stability.